Characterization of miscible poly(ethylene oxide)/ poly(phenyl methacrylate) system and the analysis of asymmetric T_g–composition dependence

E.M. Woo*, T.K. Mandal[1], L.L. Chang, S.C. Lee

Department of Chemical Engineering, National Cheng Kung University, Tainan, 701, Taiwan

Abstract

Miscibility in the binary blend comprising of semicrystalline poly(ethylene oxide) (PEO) and fully amorphous poly(phenyl methacrylate) (PPhMA) was discovered for the first time. Differential scanning calorimetry, optical and scanning electron microscopy, and infrared spectroscopy were performed to characterize and demonstrate miscibility in the PEO/PPhMA system (in amorphous domains). The glass transition behavior suggests that the intermolecular interactions between the pairs are not particularly strong. The Fourier-transform infrared spectroscopy results also revealed a weak-to-moderate interaction via the phenyl ring might be likely. The overall behavior of the blend is a miscible system with weak non-specific interactions, and the apparent asymmetry in the T_g–composition relationship has been analyzed with a detailed view of partially segregated PEO crystalline domains. © 2000 Elsevier Science Ltd. All rights reserved.

Keywords: Poly(phenyl methacrylate); Miscibility; Poly(ethylene oxide)

1. Introduction

Poly(ethylene oxide) (PEO) is a water-soluble, semicrystalline polymer. It possesses a relatively simple structure and is capable of packing into crystals, which serves as an ideal model polymer for wide variety of studies. Owing to its wide industrial applications as well as the fact that it serves as an ideal model polymer, PEO has been extensively studied. Miscibility involving PEO has been a topic of interest, and polymer blends involving poly(ethylene oxide) (PEO) have been a subject of many diversified studies. In the past decades, PEO has been found to be miscible with several polymers. Miscibility involving PEO is more commonly seen in cases where the polymer systems are capable of forming intermolecular hydrogen bonding with PEO. Examples include miscible blends of PEO with phenoxy [1], poly(acrylic acid) [2], poly(methacrylic acid) [3], etc. PEO can also be miscible in crosslinked-networks when blended and co-cured with thermosetting polymers, as illustrated in PEO-modified-crosslinked epoxy (aromatic amine cured) [4]. It is believed that an interpenetrating network (IPN) is formed with PEO dispersing in the cross-linked epoxy, and that inside the IPN networks, extensive hydrogen bonding between the ether (−O−) of PEO and −OH of epoxy chains can be expected.

Cases of miscibility in PEO blends are less reported where no specific interactions are involved between PEO and the partner polymers. The only known such miscible blend system in absence of specific interactions is the extensively studied PEO blend with poly(methyl methacrylate) (PMMA). Topics of miscible PEO/PMMA widely documented in the literature [5–11] range from the effects of casting solvents, spherulitic crystalline morphology, crystallization kinetics, thermal behavior and oxidation, interaction parameters, to IR spectroscopy and NMR studies on PEO/PMMA, etc. However, so far PEO has been found to be miscible with only PMMA, and prospect of miscibility in polymer mixtures of PEO with other types of acrylic polymers has not been discussed in the literature.

The objective of this work was to investigate other possible cases of miscibility between PEO and acrylic polymers other than PMMA. Structural window and factors influencing miscibility between PEO and acrylates were probed. Attempts were made for searching a structural window within which miscibility behavior might be located as well as the way the polymer structure might influence the interactions, phase behavior/domain, or miscibility.

---

* Corresponding author. Tel.: + 886-6-275-7575 ext. 62670; fax: + 886-6-234-4496.

E-mail address: emwoo@mail.ncku.edu.tw (E.M. Woo).

[1] Presently at Department Chemistry, Tufts University, USA.

Table 1
Absorbance of carbonyl ($>$C=O) stretching and phenyl C–H bending in PEO/PPhMA blends

PEO/PPhMA	$\nu_{>C=O}$ (stretching) (cm^{-1})	$\nu_{\phi-H}$ (bending) (cm^{-1})
0/100	1749.5	688.4
10/90	1749.6	688.6
20/80	1749.5	689.2
30/70	1749.6	689.7
40/60	1749.4	690.2
50/50	1749.4	690.3
60/40	1749.0	690.5
80/20	1749.1	691.1
100/0	–	–

2. Experimental

2.1. Materials and sample preparation

Poly(ethylene oxide) (PEO) was obtained from a specialty polymer supplier (Polysciences, Inc., USA) with $M_w = 2 \times 10^5$ g/mol, $T_g = -60°C$, $T_m = 62 - 67°C$ (manufacturer report), and it was used as-received. Poly(phenyl methacrylate) (PPhMA) is an amorphous acrylate polymer and was supplied by Scientific Polymers Product, Inc. (SP^2, USA). A wide variety of other acrylate polymers were also used in preliminary screening examination. Several solvents, including tetrahydrofuran (THF), chloroform (CCl$_3$H), and dichloromethane (CH$_2$Cl$_2$), and benzene, etc., were used for sample preparation (blending and film-casting). It was determined that benzene yielded the best result for blending PEO and PPhMA. Use of other solvents might easily lead to kinetically induced phase separation. The polymers were first weighed respectively and dissolved into the solvent (benzene) with continuous stirring at slightly elevated temperatures. Subsequently, the resulting polymer solution after complete dissolution and mixing was poured into an aluminum film-mold kept at 60°C. The solvent in the cast-film samples was first vaporized under a hood at a controlled temperature, followed by final solvent removal in a vacuum oven for 72 h at 60–70°C.

2.2. Apparatus

Fourier-transform infrared spectroscopy (FTIR, Nicolet Magna-560) was used for investigating possible molecular interactions between the constituents. Spectra were obtained at 2 cm^{-1} resolution and averages of spectra were obtained from at least 64–200 scans (for enhanced signal) in the wavenumber range of 400–4000 cm^{-1}. The blend samples were cast as thin films of uniform thickness directly on KBr pellets kept at 45°C. Subsequently, the IR measurements were performed on the KBr-cast film samples at ambient temperature. The glass transition temperatures and other thermal transitions of neat polymers and their blends were measured with a differential scanning calorimeter (Perkin–Elmer DSC-7) equipped with a mechanical intracooler (with

circulation coolant down to $-60°C$)). Sub-ambient DSC runs (temperatures lower than $-60°C$) were cooled with a liquid nitrogen tank and helium gas purge. DSC instrument was re-calibrated for the set-up with liquid nitrogen cooling. All T_g measurements were made at a scan rate of 20°C/min, and T_g was taken as the onset of the transition (the change of the specific heat) in the DSC thermograms.

Morphology (fracture surface) of blends was examined using a scanning electron microscope (SEM, Model JEOL JXA-840). The blend film samples for scanning electron microscopy were solution-cast (on proper tools) to be thick enough so that fracture surface of the thickness (cross section) could be conveniently examined. The fractured surfaces of the blend samples were coated with gold by vapor deposition using vacuum sputtering. In addition, a polarized-light optical microscope (Nikon Optiphot-2, POL) was used for examining preliminary phase structure as well as heat-induced phase transitions (crystallization, melting, cloud point, etc.). The blends were cast as thin films on glass slides, dried properly in a temperature-controlled oven before they were examined using the optical microscope. For comparison, samples for optical examination were prepared using the same solvents and casting temperature as those used in preparing the thermal analysis samples. Cloud point measurement of the blends was performed by placing the samples on a microscope heating stage (temperature-programmed), with a programmed heating rate of approximately 2°C/min from room temperature up to 300°C.

3. Results and discussion

3.1. Molecular interactions by IR

Table 1 lists the peak positions of IR absorbance for the phenyl C–H bending (in PPhMA) and C=O stretching (in PPhMA) for the PEO/PPhMA blend system. Examination was on possible interactions through the functional ether group in PEO and the pendant carbonyl group in the acrylate polymer. Likelihood of intermolecular interactions through the ether group of PEO and the phenyl group or carbonyl group of PPhMA was examined. The C–H (phenyl) bending absorbance was found at 688.4 cm^{-1} (for neat PPhMA), which up-shifts to 691.1 cm^{-1} for PEO/PPhMA (80/20) blend. This up-shifting, though only about 3 wavenumbers, indicates that weak-to-moderate intermolecular interactions involving the phenyl group may be possible. On the other hand, the IR absorbance peaks of the carbonyl stretching (C=O of PPhMA) for the blend of various compositions were found to be almost stationary at 1749.1–1749.5 cm^{-1}. Obviously, no noticeable C=O peak shifting with respect to composition can be noted, which suggests that intermolecular interactions in PEO/PPhMA, if existing, are more likely through phenyl–ether pair, rather than through the ether-carbonyl.

A. PEO/PPhMA (10/90)

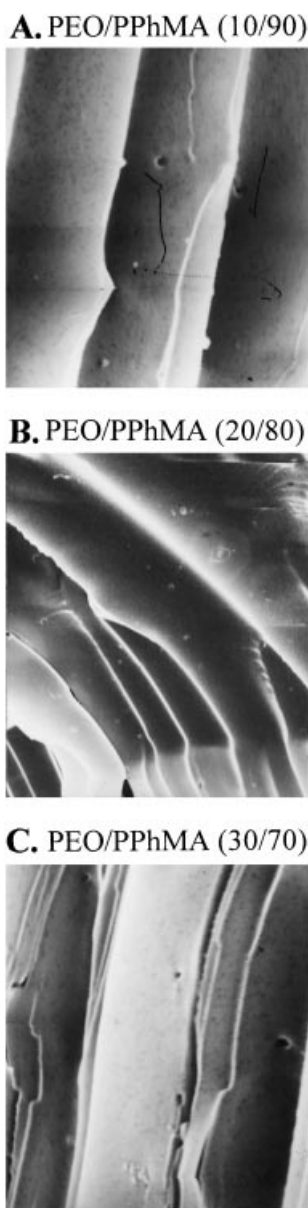## B. PEO/PPhMA (20/80)

C. PEO/PPhMA (30/70)

Fig. 1. SEM micrographs of PEO/PPhMA blend samples of three PPhMA-rich compositions: (A) 10/90, (B) 20/80, and (C) 30/70 (wt. ratios), respectively.

The spectra range for the –O– group (not listed in the table) was also examined. The neat PEO exhibited triplet peaks at $1147.5 \, cm^{-1}$ (m), $1112.5 \, cm^{-1}$ (s), and $1061.5 \, cm^{-1}$ (m), while the neat PPhMA exhibited doublet peaks at $1175 \, cm^{-1}$ (w) and $1143 \, cm^{-1}$ (s), for the ether group, where the symbols (w), (m), and (s) indicate weak, medium, and strong absorbance, respectively. The PEO/PPhMA blend compositions exhibited all five peaks. The $1147.5 \, cm^{-1}$ (m) and $1126.5 \, cm^{-1}$ (s) peaks (–O– in PEO) for the blends (50/50 composition) were observed to down-shift by about $2 \, cm^{-1}$, but the $1061 \, cm^{-1}$ peak remained at the same position for the 50/50 blend composi-

tion. It was determined that the observed "down-shifting" for the 1147.5 and 1126.5 peaks of PEO ether most likely was a result of overlapping with the $1143 \, cm^{-1}$ peak of the PPhMA ether group. The $1061.5 \, cm^{-1}$ peak of PEO is not overlapped with the PPhMA ether, and it remains at the same position for the blends. As both polymers contain the same –O– group, and the spectra show that the corresponding absorbance peaks are overlapped for the blends. The shifting is more likely caused by peak overlapping in the blends and could not be used as clear evidence of any interactions between the –O– groups or between the PEO ether and PPhMA carbonyl group. Miscibility in PPhMA and PEO as a result of a match of molecular polarity may be a plausible factor. Observation of lacking any specific interactions in PEO–PPhMA system is quite similar to the extensively studied PEO–PMMA blend system. Martuscelli et. al. [12] concluded that intermolecular interactions between molecules of PEO and PMMA in blends are very weak and their miscibility depends only "physical" van der Waals type interactions, and that specific interactions in PEO–PMMA are non-existent.

3.2. Phase morphology and structure

The cast films of all PEO/PPhMA compositions were examined using POM, which revealed apparently clear and homogeneous structure at above the melting temperature of PEO. Blends with PPhMA-rich compositions contained virtually no PEO crystals, and these blend samples at ambient temperature were clear and free of any heterogeneous domains when examined using the optical microscope at the maximum magnification (not shown here for brevity). In addition, to monitor cloud-point transition in this polymer mixture system, optical clarity of the samples of various compositions with respect to temperature was inspected at step-wise elevating temperatures up to degradation temperatures (250°C or above). Beyond 250°C, the polymers degraded rapidly and LCST could not be observed. To sum up, the result showed no cloud point phenomenon associated with the lower critical solution temperature (LCST) up to the experimentally accessible temperature of 250°C for the PEO/PPhMA blend.

In addition to the optical microscopy characterization on the phase homogeneity, blend morphology was also observed using SEM. Experimental difficulty was expected and indeed encountered. This was because the blend samples of compositions containing higher contents of PEO were not suitable for SEM characterization because of low melting temperatures of PEO, which melted easily during vacuum-sputtering coating and led an altered morphology in the blend samples. To avoid complication from low-melting PEO crystals in blends, only samples of PPhMA-rich compositions were characterized using SEM. Fig. 1 shows the SEM micrographs of three representative PEO/PPhMA blend samples: (A) 10/90, (B) 20/80, and
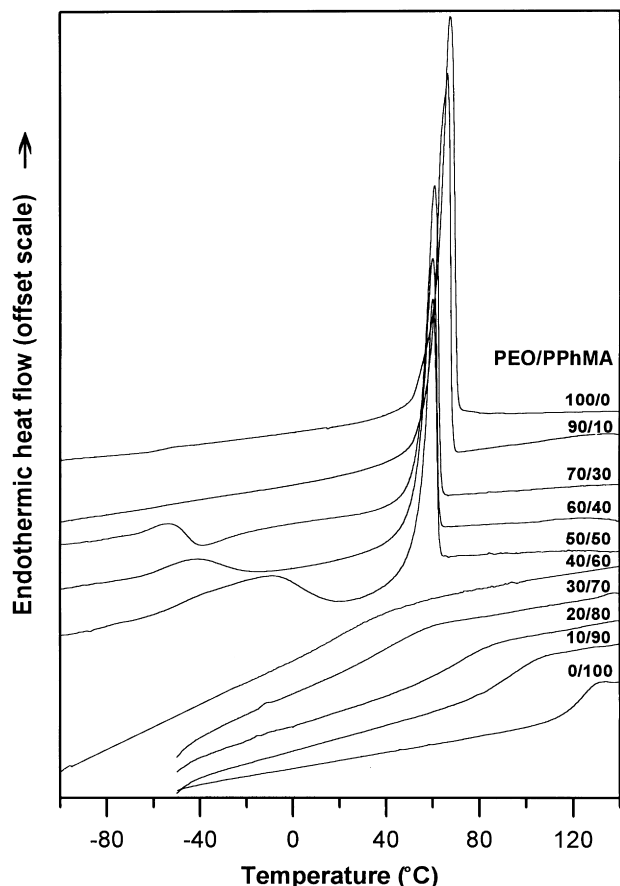
Fig. 2. DSC thermograms revealing a single T_g for PEO/PPhMA blends of several different compositions, as indicated. T_g broadening for some intermediate compositions is noted.
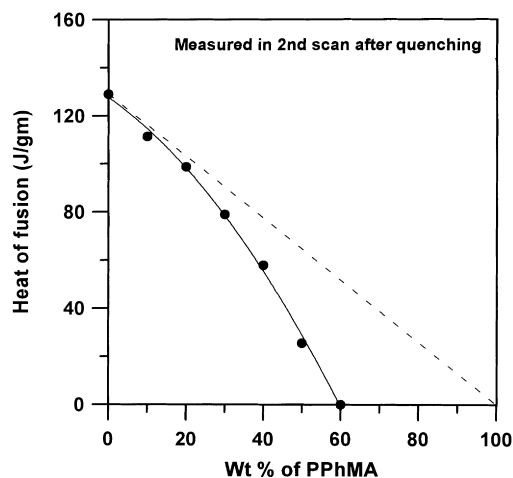

Fig. 3. Heats of fusion (ΔH_f) as a function of weight % of PEO in the blend samples subjected to DSC scanning at 10°C/min.

(C) 30/70 (wt. ratios), respectively. Therefore, SEM characterization of phase morphology was demonstrated on the fully amorphous PEO/PPhMA blend compositions. The three graphs clearly show no discernible heterogeneity in these samples. The SEM result provides additional supportive evidence on phase homogeneity in this blend system.

3.3. Single glass transition

Single T_g with a reasonable transition breadth is a generally acceptable criterion for phase homogeneity in polymer mixtures. DSC analysis was performed on the PEO/PPhMA samples to reveal their glass transition behavior. For uniformity of thermal history imposed on all blend samples, the DSC thermograms are results of second runs after quenching from temperatures just above T_g of the higher-T_g component, PPhMA. Fig. 2 shows DSC thermograms revealing one composition-dependent T_g for PEO/PPhMA blends of a wide range of compositions, as indicated in the curves. The thermograms clearly show that although there may be some broadening trend for intermediate blend compositions, there is only one T_g for each composition and that the only T_g is composition-dependent. The broadening phenomenon suggests that various scales of molecular micro-phase heterogeneity might exist in intermediate blend compositions. The micro-phase heterogeneity, however, is not significantly enough to cause phase separation that can be detected by DSC analysis. The DSC thermograms showed some extent of T_g broadening for several middle compositions (near 50/50). Note that similar broadening phenomena have also been observed in many miscible blend systems whose miscibility occurs in absence of any strong specific interactions or whose constituent polymers only possess relatively weak polar interactions. The T_g broadening phenomenon suggests that the scale of mixing might have a limit, and that various scales of molecular aggregation might exist. The term "aggregation" here means segmental neighboring of same-polymer molecules (or segments) in a large domain or in a greater probability than that of different kinds.

The crystallization tendency is usually suppressed in miscible blend systems comprising of a semicrystalline polymer and an amorphous polymer. In this study, heats of fusion in the PEO/PPhMA blends were examined to yield clues of extend of inter-molecular interactions. Fig. 3 shows the heats of fusion (ΔH_f) for PEO/PPhMA blends as a function of weight % of PPhMA in the quenched blend samples subjected to second DSC scanning at 10°C/min after quenching. Apparently, the figure shows a negative deviation from linearity is observed, which may be attributed to the disruption of the crystallizing PEO polymer chains by the favorably interacting amorphous polymer (PPhMA) chains. For weak inter-segmental interactions, effect of amorphous PPhMA on suppressing the PEO crystallization tendency may be only moderate but is clearly evident. The
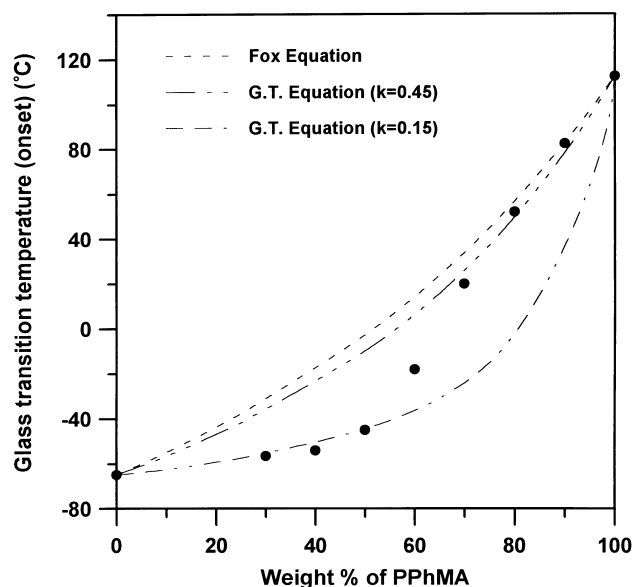
Fig. 4. Plot of T_g vs. composition of PEO/PPhMA in the whole composition range. Asymmetric composition dependence is noted.

figure shows that the relationship is almost linear only up to 80/20 composition (i.e. 20 wt% PPhMA). However, a further increase in the PPhMA content in the PEO/PPhMA blend was found to depress the crystallization tendency of PEO, leading to an increasingly noticeable negative deviation from linearity. Disruption of PEO crystallization by PPhMA is seen to increase for greater contents of PPhMA in the blends (70/30, 60/40, and 50/50). Beyond the 50/50 composition, a further increase of PPhMA over 50 wt% is seen to entirely suppress the PEO crystallization. The figure shows that at 60 wt% PPhMA (or greater), the blend samples exhibit no melting enthalpy, suggesting that PEO did not crystallize and the PEO/PPhMA blend samples were completely amorphous. Note that such behavior has also been illustrated, for examples, in the miscible poly(ε-caprolactone) (PCL) blend with poly(vinyl chloride), which shows a significantly disturbed (depressed) crystallization tendency of PCL in miscible PCL/PVC blend, presumably by favorable molecular/segmental polarity interactions [13].

3.4. The T_g–composition dependence

A quantitative evaluation of the T_g–composition relationship of a miscible blend may provide some tip of the scale of blend homogeneity. The quantitative analysis is usually done via classical T_g–composition models for homogeneous polymer mixtures. Fig. 4 shows the quantitative trend of T_g variation with composition, where the onset T_g of each blend was plotted as a function of composition. Fitting of the T_g data with several common models for miscible polymer systems was examined. In the same figure, data fitting was

also compared to the classical Fox model [14]:

$$1/T_g = \omega_1/T_{g1} + \omega_2/T_{g2}. \tag{1}$$

Although the T_g data of the upper portion (PPhMA-rich blend samples) are not too far away from the Fox prediction, the lower portion (T_gs of PEO-rich compositions) exhibits a large negative deviation from the Fox equation. Overall, a significant asymmetry in the T_g-composition relationship is apparent. Then, two T_g models with an adjustable parameter were examined: the Gordon–Taylor (G–T) or Couchman model. The Gordon–Taylor equation (or equivalently the Kelley–Bueche model if volume fraction is used instead) was first used for fitting with data [15]:

$$T_g = (\omega_1 T_{g1} + k\omega_2 T_{g2})/(\omega_1 + k\omega_2) \tag{2}$$

where ω_i is the mass (weight) fraction of the ith polymer component, and $k = \Delta C_{p2}/\Delta C_{p1}$, i.e. ratio of heat capacity change of PEO polymer ($T_{g1} = -65°C$) to that of PPhMA (high-T_g component, $T_{g2} = 115°C$) at T_g. A reasonable fitting with the G–T equation could be obtained and the best fitted parametric value was found to be quite low at about $k = 0.15$–0.45, whose value depended on the ranges of the T_g-composition data. A general trend is that the value of k is lower (~ 0.15) for the PEO-rich blend compositions, but tends to be higher $k = 0.45$ for the PPhMA-rich blend compositions. The parameter (k) in either the Gordon–Taylor or Couchman equation is considered to be correlate with the intensity of interactions or state of phase homogeneity in blends [16]. This fact indicates two points. One is that the relatively low value of k suggests that the molecular interactions are not particularly strong or specific. Secondly, the changing value of k parameter suggests that the scale of phase homogeneity of the blend was likely varying with composition.

It can be argued that effect of residual PEO crystallinity might be partially responsible for the peculiar trend observed in the T_g-composition curve. This point needs to be analyzed carefully to understand exactly how it may affect the T_g-composition dependence. Within the range of PEO-rich compositions (PEO >80 wt%), PEO in blends crystallized quickly, and thus no cold crystallization of PEO was observed in the fast-quenched PEO/PPhMA blend. This suggests that PEO in blends crystallized quite rapidly and could not be made into an amorphous glass even at the fastest available quenching rates. As a result, the T_g for these PEO-rich blends was difficult to detect, owing to masking effect of PEO crystal. However, beginning at 30 wt% or higher PPhMA (i.e. PEO <70 wt%) in the PEO/PPhMA blend, the quenched blend samples upon DSC scanning exhibited an increasingly observable cold-crystallization exothermic peak, which is located immediately above the T_g transition. Blend T_g was more apparent for these compositions; however, owing to the proximity of T_g and co-crystallization transitions, the actual values of experimental T_g for these compositions (PPhMA wt% equal or greater than 30 wt% but lower than 50 wt%)

Table 2
Calculated T_g of PEO/PPhMA blends (PEO-rich compositions) in comparison with experimentally measured values (Note: (1) PEO/PPhMA blends containing PEO less than 50% remained fully amorphous (no PEO crystalline phase) regardless of quenching or not. These blends are thus not included in this table for comparison. (2) The calculated T_g was obtained by assuming residual PEO crystal phase is excluded from the miscible amorphous region. Measured T_g, heats of fusion, and crystallinity of blends are also listed for comparison)

PEO/PPhMA (wt ratio)	ΔH_f (J/g, blend)	ΔH_f (J/g PEO)	Crystallinity[a] (% in PEO)	Cal. T_g in amor. region (°C)	Exp. T_g (°C)
100/0	129.4	129.4	59.7	−65.0	−65.0
90/10	111.4	123.7	57.3	−46.4	(∼−65)[b]
80/20	98.8	123.5	57.2	−28.1	(∼−60)[b]
70/30	78.9	112.7	52.2	−13.9	−57.1
60/40	57.8	96.3	44.6	−2.6	−54.3
50/50	25.5	51.2	23.6	0.8	−46.2

[a] Expressed as % crystal in the PEO component, by considering $\Delta H_f^0 = 216$ J/g for perfectly crystalline PEO.
[b] Numbers within parenthesis ( ) indicate the values that were hard to obtained experimentally owing to high percentage of unsuppressed residual PEO crystals in blends.

might have been higher than otherwise. With further increase of PPhMA in the PEO/PPhMA blend, the scanning-induced cold-crystallization in the quenched blends became gradually more pronounced. For those with even higher PPhMA contents (near 50 wt%), the crystallization tendency of PEO in the blends can be completely suppressed. Eventually for those with PPhMA contents greater than 50 wt%, the crystallization tendency of PEO in the blend was found to be completely suppressed.

As the T_g-composition relationship applies to the amorphous region of the blend only, the residual crystalline phase must be excluded. Formula for calculating the relative PEO/PPhMA fractions in the amorphous region of the blend (i.e., excluding PEO crystal) can be written as:

$$X_c \omega_1 (\text{crystallinity in blend}) = \Delta H_f^{bl} / \Delta H_f^0 \quad (3)$$

where ω_1 is the weight fraction of PEO (semicrystalline) polymer in the blend, and ω_2 is the weight fraction of PPhMA (all amorphous) polymer in the blend; X_c is the crystallinity of PEO crystalline phase in the PEO polymer; ΔH_f is the measured melting enthalpy of blend samples; and $\Delta H_f^0 = 216$ J/g (fusion enthalpy of perfectly crystalline PEO). The fraction of "amorphous PEO" in the total blend (amorphous PEO/PPhMA domain + crystalline PEO phase domain) can be obtained from a mass balance, as following:

$$\omega_{1,amor} = \omega_1 (1 - X_c) \quad (4)$$

If one excludes the PEO crystals from the blend, the fraction of amorphous PEO in the amorphous region of the blend is ω_1':

$$\omega_1' = \omega_{1,amor} / (\omega_2 + \omega_{1,amor}) \quad (5)$$

The weight fraction of PPhMA in the amorphous region of the blend is then $\omega_2' = 1 - \omega_1'$. That is, if one takes into account that the crystalline portion of PEO does not participate in blending, the actual PPhMA fraction (ω_2') is higher than the blending compositions (ω_2). Conversely, the actual amorphous PEO fraction (ω_1') in the amorphous region of

the blend tends to be lower than the blending composition (ω_1).

With these re-adjusted PEO/PPhMA compositions (ω_1', ω_2'), one then estimates the anticipated T_g of the blend by assuming that a well-miscible amorphous PEO/PPhMA phase in the PEO-rich blends (semicrystalline) should behave nearly similarly to those PPhMA-rich blends (completely amorphous). The T_g of these PEO-rich blends was calculated using the re-adjusted compositions according to the demonstrated valid model for the upper portion (amorphous PPhMA-rich blend compositions) of the T_g–composition relationship. shows the comparison of experimental measured T_g (for PEO-rich blend compositions only) and calculated T_g by assuming that the PEO crystalline phase does not participate in blending in the amorphous region. Note that the blends of PPhMA-rich compositions (PPhMA >50 wt%) remained amorphous and no PEO crystalline phase was detected, and the compositions in the amorphous region of the blend was not influenced by PEO. The experimentally measured T_gs of the PEO-rich blend compositions are much lower than the expected T_gs calculated using the re-adjusted compositions (ω_1', ω_2'). The calculated T_gs (listed in Table 2) are near or at slightly above the Fox model prediction, in comparison to the experimentally measured T_gs skewed at much lower temperatures.

Thus, with the re-adjusted compositions by excluding the portion of residual PEO that may have remained crystalline upon fast quenching, the origin of asymmetric dependence still could not be accounted for. A somewhat peculiar trend is that T_g (on-set) of the PEO/PPhMA blends initially increases sluggishly with increasing PPhMA. That is, initially at low PPhMA contents (i.e. PEO-rich, e.g. PEO >60 wt%), there exists a leveling trend in the T_g-composition curve where an increase in PPhMA content does not seem to lead to proportional increase in the blend's T_g. More steady increase of blend T_g is observed only in the range of PPhMA-rich contents in the blend. More thorough analysis for explaining the phase behavior in association with the T_g behavior has to be provided in more details.
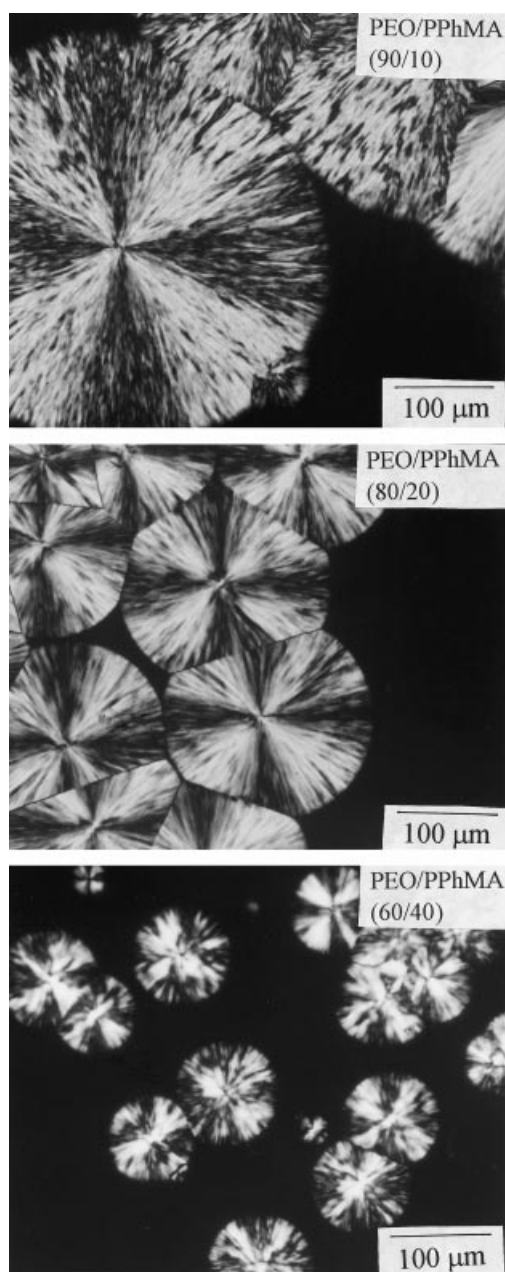
Fig. 5. POM micrographs showing presence of crystalline PEO phases before melting and quenching in PEO/PPhMA blends. Three representative compositions: 90/10, 80/20, and 60/40.

Fig. 5 shows the actual spherulite morphology of PEO/PPhMA blends (PEO contents greater than 60%) with extensive crystalline PEO phases in PEO/PPhMA before melting. Note that the spherulites as shown are not three-dimensional uniform in dimensions, as the cast film (on glass slides) was only about $15–20 \, \mu m$ in thickness but the spherulites in the cast blend samples ranged from 100 to $200 \, \mu m$. The spherulties were in effect spread out or plane-stretched when cast as films. The actual dimensions of PEO spherulites in bulk were expected to be smaller. Nevertheless, the as-grown PEO spherulites are relatively

larger when compared to those in other semi-crystalline polymers.

Apparently, the residual crystallinity is not (entirely) responsible for the variation of T_g–composition behavior. The lack of agreement between T_g and the models, especially for the PEO-rich compositions after taking into account the crystallinity adjustment required some more in-depth probing. Obviously, for PEO-rich blend compositions, PEO crystalline domain may exist persistently. PEO crystallinity in blends could be depressed by fast-quenching in DSC or by dipping into liquid nitrogen. Upon heating a blend to above PEO T_m ($\sim 65°C$), the spherulites would melt into a liquid aggregate of PEO domain. However, with the relatively large spherulite domains, there might be kinetic hindrance for the melted PEO chains to readily mix with the neighboring PPhMA moleucles, originally located outside the PEO spherulites. By comparison, mixing at above T_m between PEO and PPhMA moelcules might be kinetically less hindered for the PPhMA originally trapped within the PEO lamellar bundles. The amount of PPhMA in inter-lamellar regions available for ready mixing, however, is relatively less in comparison with those outside the spherulites.

It is thus proposed that that the residual undisturbed crystal domains may obscure the T_g determination for the PEO-rich blend compositions. To illustrate this point, a schematic based on the above spherulite morphology for the PEO-rich blends is drawn. Fig. 6 shows schematics of partially solidified and still-segregated PEO domains upon melting and quenching to about $-80°C$ prior to DSC scanning for blend T_g characterization. Unless the PEO crystals could be melted and thoroughly mixed in molten state with the PPhMA polymer chains prior to quenching, a PEO segregated domain is bound to exist, leading to an almost stationary T_g that reflects a partially segregated PEO phase. Although all blend T_gs were measured on second scanning after melting the PEO crystals at ca. 120°C and fast quenching to $-80°C$ prior to DSC measurements, the melted PEO domains are somewhat isolated as a result of the stated reason. Certainly, at above the T_m, diffusion and intermixing occur more readily between melted PEO and PPhMA chains, especially in regions of immediate interfaces. But the relative large sizes of PEO spherulites and lamellae bundles (see Fig. 5) may hinder the intermixing process from going to inner domains. Such asymmetry of T_g-composition relationship may occur in miscible semicrystalline/amorphous blends as well as in amorphous/amorphous blend systems. In amorphous/amorphous blends, the asymmetry may infer a composition dependence of interactions and/or variation of scales of phase homogeneity. In semicrystalline/amorphous blends, the asymmetry may be further complicated by contribution owing to the segregated crystalline phase remaining unmixed. Note, however, that not all miscible semicrystalline/amorphous blends exhibit asymmetric T_g-composition dependence [17,18].
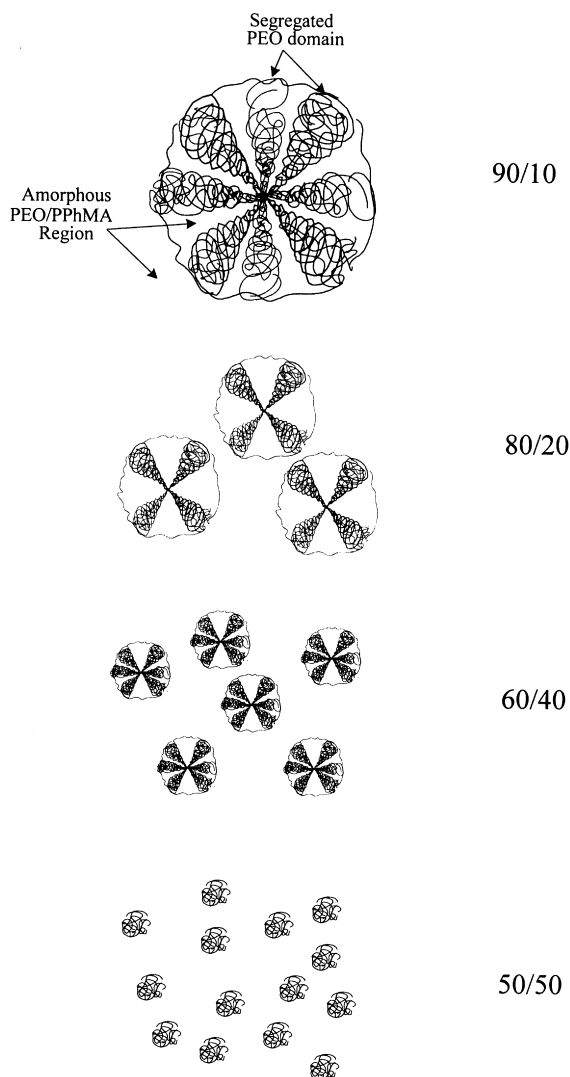
Fig. 6. Schematics showing segregated PEO domains upon melting and quenching prior to DSC scanning for T_g characterization of PEO/PPhMA blends.

4. Conclusions

This study has, for the first time, discovered miscibility in the binary blend of PEO and PPhMA (excluding the PEO crystalline phase) according to all conventional criteria. The FTIR characterization revealed slight shifting of the phenyl C–H bending vibration, suggesting that weak interactions might be involved. Other than the barely noticeable interaction via phenyl ring, the miscibility in PEO and PPhMA may be primarily attributed to physical polar–polar interactions. The homogeneous morphology of PEO/PPhMA was also revealed by SEM characterization. The asymmetry in the T_g–composition relationship was analyzed with a detailed view of partially segregated PEO crystalline domains.

References

[1] Robeson LM, Hale WF, Merriam CN. Macromolecules 1981;14:1644.
[2] Smith KL, Winslow AE, Peterson DE. Ind Engng Chem 1959;51:1361.
[3] Osada Y, Satam M. J Polym Sci Polym Lett Ed 1976;14:129.
[4] Horng TJ, Woo EM. Polymer 1998;39:4115.
[5] Li X, Hsu SL. J Polym Sci Polym Phys Ed 1984;22:1331.
[6] Calahorra E, Cortazar M, Guzman GM. Polymer 1982;23:1322.
[7] Martuscelli E, Vicini L, Seves A. Makromol Chem 1987;188:607.
[8] Runt JP, Barron CA, Zhang XF, Kumar SK. Macromolecules 1991;24:3466.
[9] Alfonso GC, Russell TP. Macromolecules 1986;19:1143.
[10] Bartczak Z, Martuscelli E. Makromol Chem 1987;188:445.
[11] Martuscelli E, Silvestre C, Addonizio ML, Amelino L. Makromol Chem 1986;187:1557.
[12] Rao GR, Castiglioni C, Gussoni M, Martuscelli E, Zerbi G. Polymer 1985;26:811.
[13] Khambatta FB, Warner F, Russell T, Stein RS. J Polym Sci Polym Phys Ed 1976;14:1391.
[14] Fox TG. Bull Am Phys 1956;2:123.
[15] Gordon M, Taylor JS. J Appl Chem 1952;2:493.
[16] Prud'homme RE. Polym Engng Sci 1982;22:90.
[17] Mandal TK, Woo EM. Polym J 1999;31:226.
[18] Tseng YC, Woo EM. Macromol Rapid Commun 1998;19:215.